Available online at www.sciencedirect.com

ScienceDirect

journal homepage: www.elsevier.com/locate/he

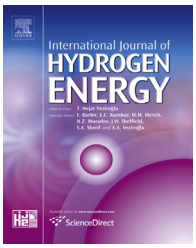

An experimental investigation of biodiesel steam reforming

Stefan Martin [a,*], Gerard Kraaij [a], Torsten Ascher [a], David Wails [b], Antje Wörner [a]

[a] German Aerospace Center (DLR), Institute of Technical Thermodynamics, Pfaffenwaldring 38 – 40, 70569 Stuttgart, Germany

[b] Johnson Matthey Technology Centre, Blount's Court Sonning Common, Reading, RG4 9NH, United Kingdom

ARTICLE INFO

Article history:
Received 29 July 2014
Received in revised form
1 October 2014
Accepted 30 October 2014
Available online 24 November 2014

Keywords:
Hydrogen
Biodiesel
Steam reforming
Liquid fuels

ABSTRACT

Recently, liquid biofuels have attracted increasing attention as renewable feedstock for hydrogen production in the transport sector. Since the lack of hydrogen infrastructure and distribution poses an obstacle for the introduction of fuel cell vehicles to the market, it is reasonable to consider using liquid biofuels for on-board or on-site hydrogen generation. Biodiesel offers the advantage of being an environmentally friendly resource while also having high gravimetric and volumetric energy density.

The present study constitutes an experimental investigation of biodiesel steam reforming, the main emphasis of which is placed on finding optimum operating conditions in order to avoid catalyst deactivation. Temperature was varied from 600 °C to 800 °C, pressure from 1 bar to 5 bar and the molar steam-to-carbon ratio from 3 to 5. Based on the experimental results, coke formation and sintering are identified as the main deactivation mechanisms. Initiation of catalyst deactivation primarily depends on catalyst inlet temperature and feed mass flow per open area of catalyst. By using a metallic based precious metal catalyst, applying low feed flow rates (31 g/h·cm^2) and a sufficiently high catalyst inlet temperature (>750 °C) coking can be minimized, thus avoiding catalyst deactivation. A stable product gas composition close to chemical equilibrium has been achieved over 100 h with a biodiesel conversion rate of 99%.

Introduction

Today, approximately 65 million tons of hydrogen are produced annually worldwide [1]. Steam reforming of natural gas is the prevalent hydrogen production technology. Large quantities of hydrogen are needed in the chemical and petrochemical industry, in particular for ammonia production, oil refining and methanol synthesis. Moreover, hydrogen is increasingly discussed as a fuel for transport applications [2]. Especially production from logistic fuels is considered as a viable option to accelerate market introduction of hydrogen as an alternative energy carrier [1].

Auxiliary power units (APUs) for on-board power generation based on liquid fuels are generally regarded as one important early market for fuel cells (FCs) in transport. Detailed analysis of the market for diesel proton exchange membrane (PEM) fuel cell APUs revealed a market demand for

* *Corresponding author*. Tel.: +49 711 6862 682; fax: +49 711 6862 665.
E-mail address: stefan.martin@dlr.de (S. Martin).

http://dx.doi.org/10.1016/j.ijhydene.2014.10.143

implementation in long-haul trucks in particular in the United States and elsewhere [3]. On-board APU systems can help reduce greenhouse gas emissions. By coupling fuel processor systems based on liquid fuels with solid oxide fuel cell (SOFC) or PEM based APUs, CO_2 emissions can be reduced by up to 33% [4]. Apart from directly coupling a fuel processor with an FC, reforming of liquid biofuels can be applied for on-site decentralized hydrogen production, for instance by integrating a reformer system into an existing refueling station as currently investigated in the FCH JU project NEMESIS2+ (New Method for Superior Integrated Hydrogen Generation System 2+). Thereby problems related to the lack of hydrogen infrastructure can at least be partly avoided [5].

Recently, biodiesel has been attracting increasing attention as a renewable and environmentally friendly resource for fuel cell applications [6,7]. Currently, biodiesel is produced at a rate of approximately 30 billion liters per year, thus representing 19% of world's biofuel production [8]. Biodiesel is a fatty acid methyl ester (FAME) which is produced from transesterification of vegetable oil with methanol. Glycerol emerges as by-product and can be further used for food industry and pharmaceutical applications.

Hydrogen production from biodiesel by means of reforming can be achieved via partial oxidation (POX), steam reforming (SR) or autothermal reforming (ATR). SR is the most established technology among the available reforming options. A main advantage of SR is the high partial pressure of hydrogen in the reformate gas, which allows the subsequent fuel cell stack to operate with higher efficiency. In contrast, the system complexity of an SR-APU system is higher compared to an ATR-APU system resulting in increased system weight, volume and costs. Regarding net electrical efficiency, simulation studies of Specchia et al. and Martin et al. report comparable values for SR- and ATR-APU systems in the range of 30–39 % [9,10].

Various types of catalysts appear suitable for biodiesel reforming, including noble, non-noble and bimetallic catalysts [1,11]. Rh and Ni catalysts are commonly considered to be most suitable for steam reforming of liquid fuels [12]. The main challenge related to biodiesel reforming is unwanted coke deposition on the catalyst surface, resulting in performance losses. Furthermore, catalyst deactivation can be caused by sintering and/or sulfur poisoning [13]. Taking into account that biodiesel has a relatively low sulfur content of typically <5 ppm, coking and sintering are considered to be the main causes of catalyst deactivation.

The reported literature treating hydrogen production from biodiesel is almost entirely related to the ATR of biodiesel for fuel cell applications [14–21]. Although promising concepts have been identified, challenges remain with regard to incomplete biodiesel conversion, formation of higher hydrocarbons, catalyst coking and poor mixing of reactants. In contrast, hydrogen production from biodiesel by means of steam reforming is very recent and offers significant room for further development [6,7].

Nahar carried out a thermodynamic analysis of biodiesel SR and ATR using Gibbs free energy minimization method [22]. The water-biodiesel molar feed ratio (WBFR) was varied between 3 and 12, oxygen-biodiesel molar feed ratio (OxBFR) between 0 and 4.8 and reaction temperature between 300 °C and 800 °C at atmospheric pressure. Hydrogen yield and selectivity were found to be highest for SR conditions with a maximum hydrogen yield at WBFR = 12 and T = 800 °C. Increased coke selectivity is reported for SR compared to ATR conditions.

Martin and Wörner report a plateau for thermal hydrogen efficiency for a heat integrated biodiesel SR system (including water gas shift and burner) of 76% at S/C = 3 in the temperature range 700 °C–850 °C [10].

Abatzoglou et al. investigated biodiesel steam reforming using a newly developed Al_2O_3/YSZ supported $NiAl_2O_4$ spinel catalyst [23]. Work was performed in a fixed-bed isothermal reactor. Biodiesel/water was emulsified prior to being injected at room temperature into the reactor preheating zone maintained at 550 °C. The molar steam-to-carbon ratio (S/C) was varied between 1.9 and 2.4, the temperature between 700 °C and 725 °C and space velocity (SV) between 5500 and 13 500 $cm^3_{reac} g^{-1}_{cat} h^{-1}$ at atmospheric pressure. Results show that complete biodiesel conversion is achieved during 4 h of operation at S/C = 1.9, SV = 5500 and T = 725 °C. Coke deposition and catalyst deactivation were not observed.

Shiratori et al. evaluated paper structured catalysts (PSCs) for steam reforming of biodiesel [24]. Catalytic activity of the Ni-PSC could be significantly improved by Ni–MgO loading and introducing Cs as an inorganic binder. The inorganic fiber network of the PSC with a mean pore size of 20 μm leads to an effective three-dimensional diffusion and a good dispersion of the metal catalyst particles, resulting in efficient biodiesel conversion. 50 h of biodiesel steam reforming was achieved using a Ni–MgO loaded PSC at 800 °C and S/C = 3.5 with 90% fuel conversion. Although formation of C_2H_4 could be avoided, CH_4 levels started to rise after 28 h of operation, indicating the onset of catalyst deactivation. However, Ni agglomeration and carbon deposition on the PSC were not observed. In a follow-up study, the authors evaluated SOFC performance connected with PSC in the direct feed of wet oleic fatty acid methyl ester ($C_{19}H_{36}O_2$). By application of two PSCs in series (Ni–MgO loaded and Ru-loaded $BaTiO_3$ containing PSC) prior to a single cell SOFC, stable cell voltage has been observed for 100 h at 800 °C and S/C = 2. Carbon formation was not observed on the SOFC anode surface nor on the PSCs. Data on reformate gas composition prior to the SOFC is not available [25].

Nahar and Dupont reviewed the use of steam reforming to convert liquid bio-feedstock to hydrogen-rich product gas. They consider liquid fuels to be a promising option for hydrogen production, offering a range of advantages such as existing infrastructure and high volumetric and gravimetric energy density. According to the authors, biodiesel is among the least explored liquid feedstocks for hydrogen production [6].

The objective of this paper is to evaluate biodiesel steam reforming at various operating conditions using a proprietary precious metal based catalyst. The experimental study includes variation of the reforming temperature, pressure, steam-to-carbon ratio, feed mass flow and catalyst substrate. The main emphasis is placed on finding optimum conditions for coke-free operation, thus avoiding catalyst deactivation. The initiation of catalyst deactivation is evaluated in detail including measurement of carbon deposition on the catalyst

surface and post mortem analysis (scanning electron microscopy). The present study contributes to a fundamental understanding of biodiesel steam reforming using noble-metal catalysts, which has not yet been widely explored in the literature.

Methodology

Biodiesel properties and chemical reaction system

In this study, biodiesel produced by transesterification of soybean oil (40%) and palm oil (60%) is used as a feedstock for steam reforming experiments. A selection of physical and chemical biodiesel properties is shown in Table 1. The empirical formula $C_{18.3}H_{34.8}O_2$ was derived from the fatty acid spectrum (main components: oleic acid: 34.2%, palmitic acid: 30.9%, linolic acid: 26.0%).

Taking into account that oleic acid is the dominating species in the fatty acid spectrum and considering that the molar C:H:O-ratio of the corresponding FAME methyl-oleate ($C_{19}H_{36}O_2$) is similar to the C:H:O ratio of the commercial biodiesel used in this study, methyl-oleate was chosen as a model substance for biodiesel. Steam reforming of methyl-oleate involves three independent equations, namely conversion into carbon monoxide and hydrogen (Eq. (1)), water-gas shift reaction (Eq. (2)) and methanation reaction (Eq. (3)).

$$C_{19}H_{36}O_2 + 17H_2O \rightarrow 19\ CO + 35H_2 \quad \Delta H_{298\ K} = +2645\ kJ/mol \tag{1}$$

$$CO + H_2O \leftrightarrow H_2 + CO_2 \quad \Delta H_{298\ K} = -41\ kJ/mol \tag{2}$$

$$CO + 3\ H_2 \leftrightarrow CH_4 + H_2O \quad \Delta H_{298\ K} = -206\ kJ/mol \tag{3}$$

Whilst the steam reforming reaction is strongly endothermic, the water-gas shift and methanation reactions are exothermic. Obviously, at high temperatures the overall reaction system is endothermic, thus requiring heat supply from an external heat source. The reaction products are mainly controlled by thermodynamics. High temperatures and high steam-to-carbon ratios favor high hydrogen yields. In contrast, the application of high pressure reduces the achievable hydrogen yield [13].

Apart from the main SR reactions, unwanted coking can occur (Eqs. (4)–(8)), leading to a blocking of the active sites and subsequent catalyst deactivation. Elemental carbon can be formed directly from biodiesel, carbon monoxide and methane or via polymerization of olefins/aromatics and subsequent stepwise dehydrogenation [1]. The extent of the coking reactions strongly depends on reformer operating conditions such as temperature, steam-to-carbon ratio, gas hourly space velocity, type of catalyst and reaction kinetics [26].

Table 1 – Biodiesel properties.

Property	Value	Test method
Density at $T = 15\ °C$ (kg/m^3)	878.6	EN ISO 12185
Sulfur content (ppmw)	1.5	ASTM 5453-09
Flashpoint (°C)	132.0	EN ISO 2719
Lower heating value LHV (kJ/kg)	37 790	DIN 51 900-1,3
Fatty acid methyl ester content (ma. %)	99.5	EN 14103
Methanol (ma. %)	0.09	EN 14105
Free Glycerine (ma. %)	<0.02	EN 14105

$$CH_4 \leftrightarrow C + 2\ H_2 \quad \Delta H_{298\ K} = +75\ kJ/mol \tag{4}$$

$$2\ CO \leftrightarrow C + CO_2 \quad \Delta H_{298\ K} = -172\ kJ/mol \tag{5}$$

$$CO + H_2 \leftrightarrow C + H_2O \quad \Delta H_{298\ K} = -131\ kJ/mol \tag{6}$$

$$C_{19}H_{36}O_2 \rightarrow C + H_2 + CH_4 + \ldots \quad \Delta H_{298\ K} > 0\ kJ/mol \tag{7}$$

$$\text{Olefines, Aromatics} \rightarrow \text{Polymers} \rightarrow \text{Coke}\ \Delta H_{298\ K} > 0\ kJ/mol \tag{8}$$

Experimental test set-up

A schematic of the test rig is shown in Fig. 1a. Water and biodiesel are supplied to the system by micro annular gear pumps using mass flow controllers. Biodiesel at room temperature is mixed into superheated steam ($T = 550\ °C$) and fed to the reformer where the catalytic conversion to H_2, CO, CO_2, CH_4 and H_2O takes place. Conversion of the fuel to a hydrogen rich gas is accomplished by using catalyst monoliths coated with finely distributed platinum group metals. The catalyst comprised Rh on a high surface area (140 m^2/g), alumina based mixed metal oxide support. It is coated onto the monolith at a loading of 2 g catalyst/in^3 with an overall Rh loading of 69.1 g/ft^3. Carbon deposition on the spent ceramic monoliths was measured using an elemental analyzer (EA5000, Jena Analytik). Therefore, the catalyst piece as a whole is pulverized and the deposited carbon is oxidized to CO_2, which is subsequently detected.

The catalyst monolith is mounted inside a stainless steel tube and heated by an electrical oven. By placing four thermocouples along the axis of the catalyst piece (Fig. 1b), the temperature profile can be measured over time on stream. The axial temperature profile provides valuable information on catalyst activity. Shortly after initiation of the reforming reaction, the temperature at the catalyst inlet drops due to the endothermic heat demand of the steam reforming reaction. A stable catalyst inlet temperature over time indicates stable catalyst activity, whereas a temperature increase is accompanied by a loss of catalyst performance, which can be caused by coking, sintering and/or sulfur poisoning.

Upon leaving the reformer section, water and unconverted liquid fuel are condensed in a cold trap at $T = 10\ °C$ and stored in a condensate reservoir. Before each experiment, the cold trap is filled with 100 ml of organic solvent (dodecane, mixture of isomers). The fuel conversion rate FCR (Eq. (9)) is subsequently derived from gas chromatography (GC) analysis of the organic phase that accumulates in the cold trap during the

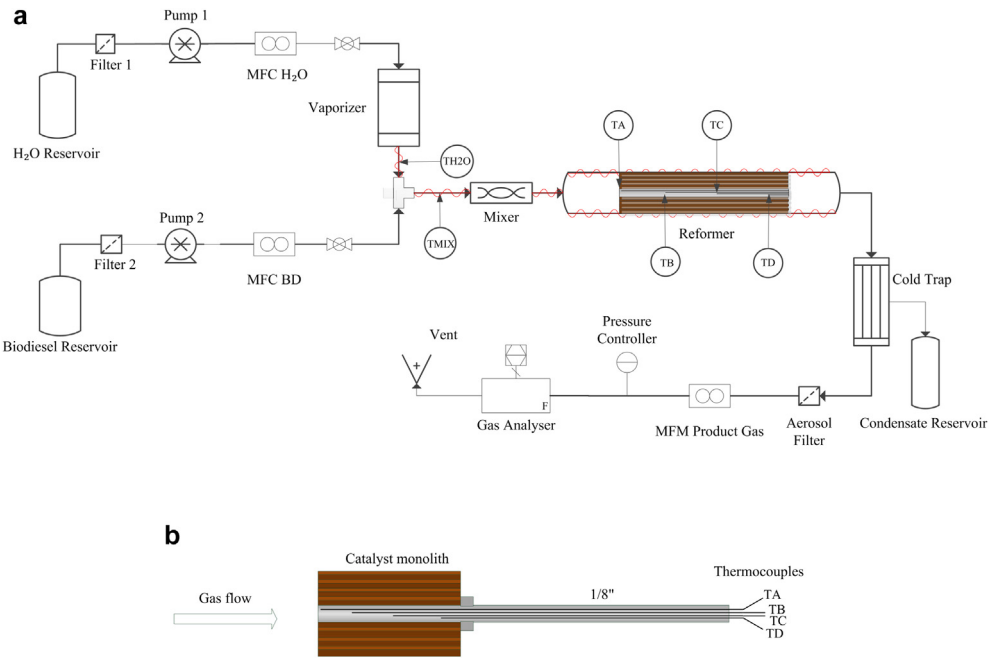

Fig. 1 – Schematic of biodiesel steam reforming test rig (a) and cross section of ceramic catalyst monolith (b).

test. GC analysis of the condensate was found to be more reliable than determining the fuel conversion via the gas phase. In addition, carbon deposition on the catalyst surface and the tube walls and higher hydrocarbons leaving the cold trap are considered for FCR calculations:

$$\mathrm{FCR} = \frac{m_{\mathrm{BD}} - \left(m_{\mathrm{BD,liq.}} + m_{\mathrm{C}} + m_{\mathrm{HCs}}\right)}{m_{\mathrm{BD}}} \tag{9}$$

The amount of condensed biodiesel and its cracking products in the cold trap $m_{\mathrm{BD,liq.}}$ is derived from the area proportion $x_{\mathrm{BD,liq.}}$ in the gas chromatogram (which is assumed to be equivalent to the mass proportion) and the amount of dodecane m_{Dod} according to Eq. (10). The amount of deposited carbon m_{C} is obtained by flushing the system with air after each test and detecting the resulting CO_2 evolution. Higher hydrocarbons m_{HCs} (C_2–C_4) passing the cold trap are measured discontinuously via GC analysis.

$$m_{\mathrm{BD,liq.}} = m_{\mathrm{Dod}} \cdot \left(\frac{1}{1 - x_{\mathrm{BD,liq.}}} - 1\right) \tag{10}$$

Subsequent to the cold trap, any remaining moisture is removed by an aerosol filter. The product gas flow is measured with a mass flow controller before it enters the online gas analyzer unit, which is equipped with an infrared absorption detector for CO, CO_2 and CH_4 and a thermal conductivity detector for the measurement of H_2. System pressure is regulated using a pressure controller.

Parameters

Thermal hydrogen efficiency based on the lower heating value (LHV) is calculated according to Eq. (11) (assuming that CO is completely converted into H_2 by means of the water-gas shift reaction):

$$\eta_{\mathrm{H_2}} = \frac{\dot{m}_{\mathrm{H_2}} \cdot \mathrm{LHV}_{\mathrm{H_2}}}{\dot{m}_{\mathrm{BD}} \cdot \mathrm{LHV}_{\mathrm{BD}}} \tag{11}$$

The gas hourly space velocity (GHSV) at standard temperature and pressure (STP) and the molar steam-to-carbon ratio (S/C) are defined as follows:

$$\mathrm{GHSV} = \frac{\dot{V}_{\mathrm{Feed,STP}}}{V_{\mathrm{cat.}}} \tag{12}$$

$$\mathrm{S/C} = \frac{\dot{n}_{\mathrm{H_2O}}}{\dot{n}_{\mathrm{BD,C}}} \tag{13}$$

Results and discussion

Tests with ceramic based catalyst monoliths

27 steam reforming experiments (test duration: 2.5 h, biodiesel mass flow: 20 g/h) with ceramic based catalyst monoliths (l: 4 cm, d: 1.8 cm) have been conducted in order to detect the influence of pressure, temperature and steam-to-carbon ratio on hydrogen efficiency and carbon deposition. Pressure has been varied in the range of 1 bar–5 bar, temperature from 600 °C to 800 °C and S/C from 3 to 5.

In line with thermodynamics, a decline of the hydrogen efficiency with increasing pressure and decreasing temperature was observed at S/C = 3 and S/C = 4 (Figs. 2a and 3a). At S/C = 5, the lower contact time seems to outweigh the effect of better thermodynamics in the low pressure range (Fig. 4a). Increasing the S/C from 3 to 5 has a positive effect on hydrogen efficiency at 600 °C, whereas the positive effect is almost negligible at 800 °C.

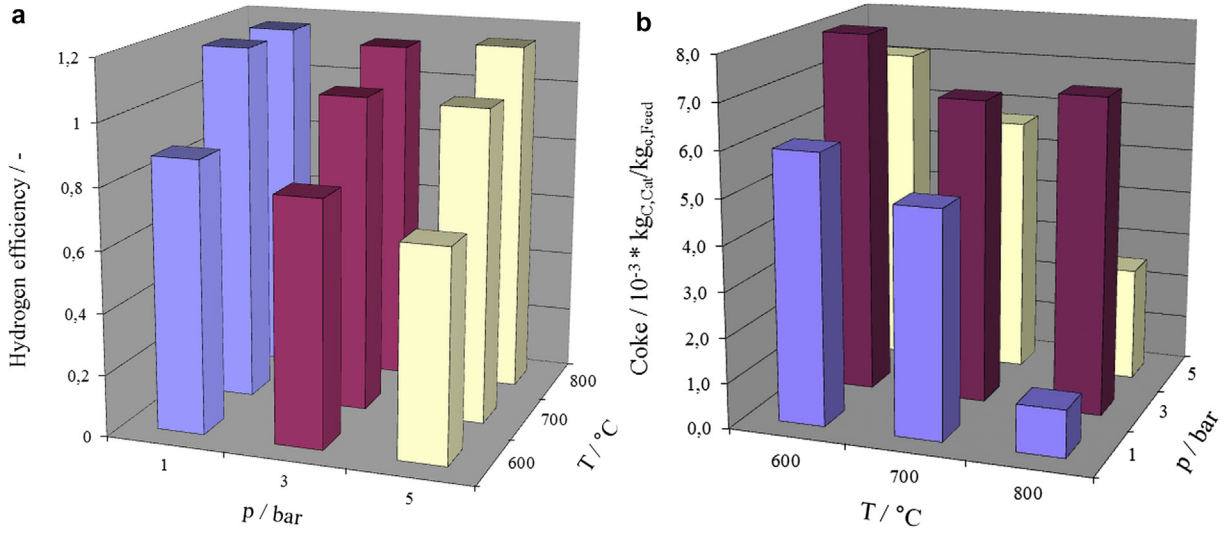

Fig. 2 – Biodiesel steam reforming: Hydrogen efficiency (a) and coke deposition (b) at S/C = 3.

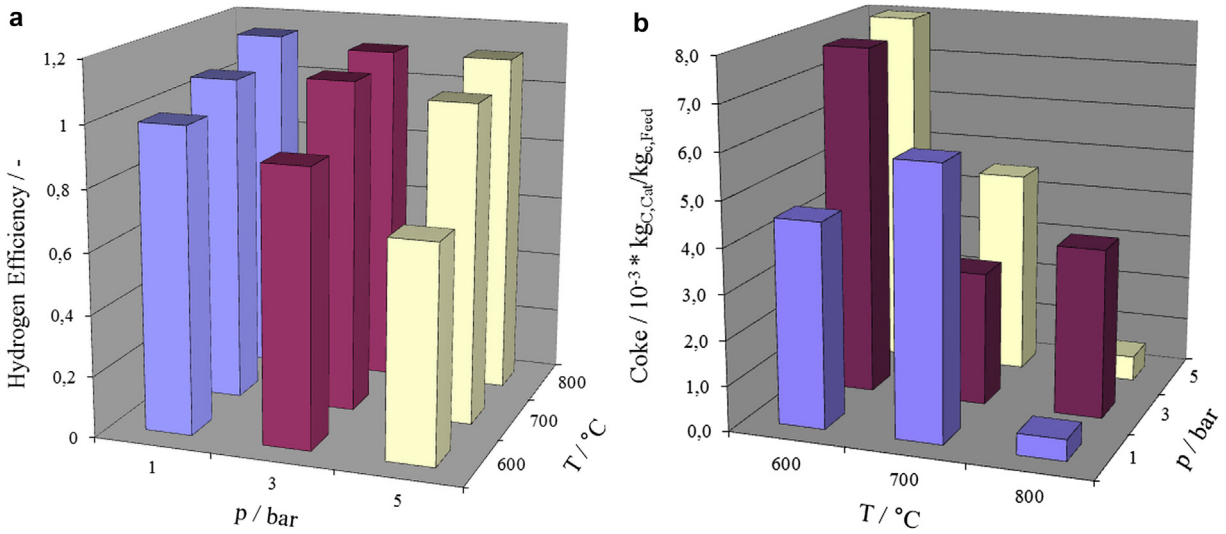

Fig. 3 – Biodiesel steam reforming: Hydrogen efficiency (a) and coke deposition (b) at S/C = 4.

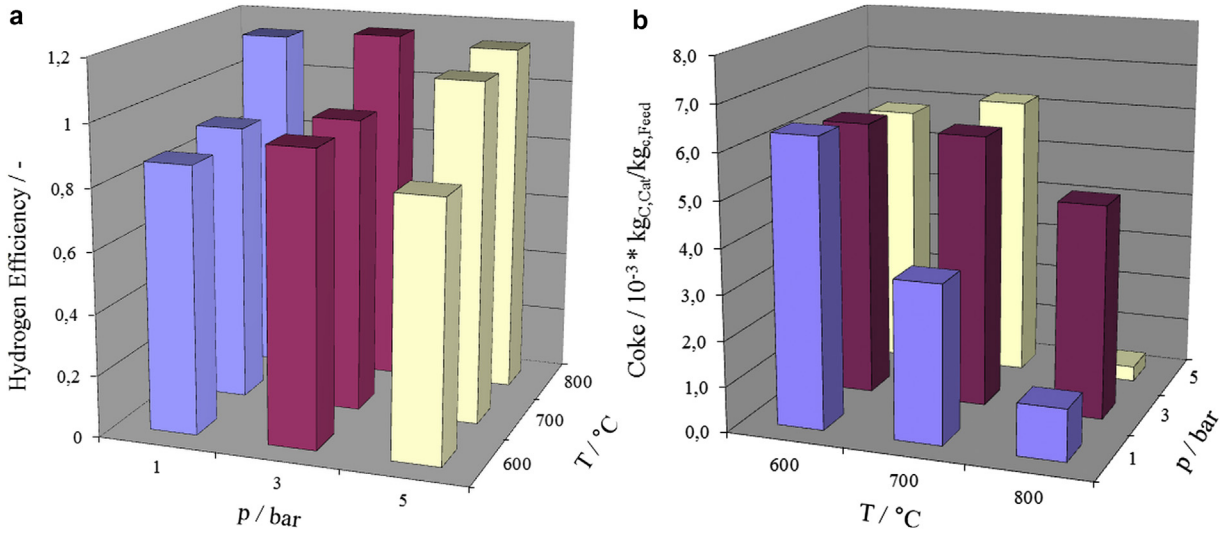

Fig. 4 – Biodiesel steam reforming: Hydrogen efficiency (a) and coke deposition (b) at S/C = 5.

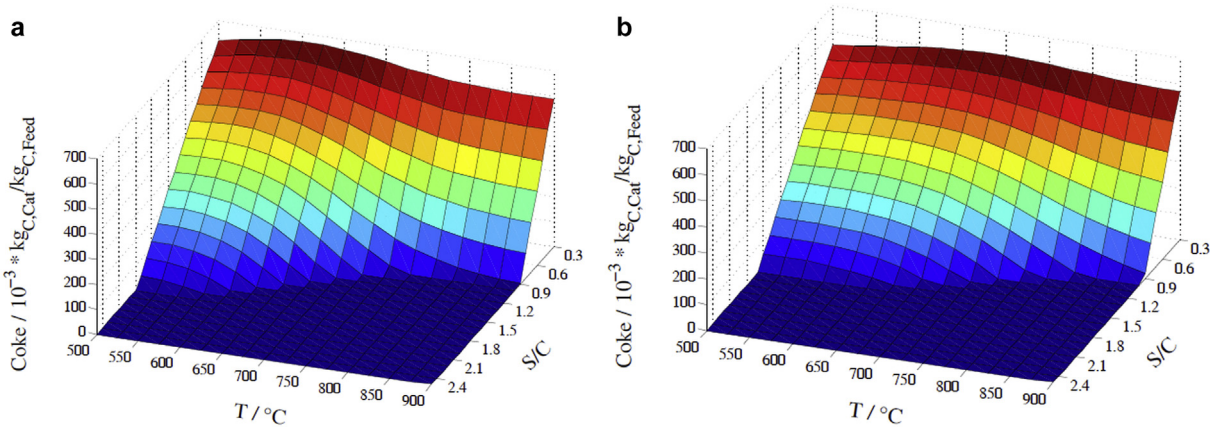

Fig. 5 – Biodiesel steam reforming: Equilibrium coke formation, a) $p = 1$ bar, b) $p = 5$ bar.

Coke deposition on the catalyst surface increases with decreasing temperature (Figs. 2b, 3b and 4b). This finding is in agreement with published literature. Lin et al. report an onset of carbon formation for ATR of biodiesel below 900 °C, accompanied by an increase in methane and ethylene production [14,27]. Concurrently, Maximini et al. observed increased carbon formation for a microchannel diesel steam reformer when reducing the temperature from 800 °C to 700 °C [28].

In line with literature findings, Aspen Plus calculations based on minimization of Gibbs free energy show increased coke formation when lowering the temperature from 900 °C to 500 °C (Fig. 5). At low S/C, coke deposition is maximal in the range of 500 °C–600 °C. The coke formation boundary at elevated pressure (5 bar) is shifted slightly towards higher temperatures and higher S/C.

Obviously, the experimentally derived coke deposition (Figs. 2b–4b) is higher than thermodynamically predicted (Fig. 5). At the given boundary conditions of the preliminary tests ($T = 600$ °C–800 °C, $p = 1$ bar – 5 bar, S/C = 3–5), carbon formation is not expected at equilibrium conditions. Similarly, Lin et al. [14] found that at S/C > 0.75 it is not possible to predict carbon formation accurately by thermodynamic equilibrium calculations. This can be attributed to heat transfer limitations in the catalyst bed and reaction kinetics, which will be discussed in more detail in chapter 3.3.

Longevity test with ceramic based catalyst monolith

Based on the preliminary experiments, a longevity test (100 h, $l = 8$ cm, d= 1.8 cm $m_{BD} = 5$ g/h) has been carried out at operating conditions where coking on the catalyst surface was found to be least severe ($T = 800$ °C, S/C = 5, $p = 5$ bar). Although a stable product gas composition close to chemical equilibrium could be achieved (Fig. 6), the axial temperature profile changed significantly over time on stream (Fig. 7). Fluctuations of axial temperatures are caused by pressure fluctuations which are induced by periodical condensate release. After the start of the reforming reaction, the catalyst inlet temperature TA drops from 800 °C to 723 °C due to the required endothermic heat demand. Shortly afterward, TA starts to rise indicating a severe loss of catalyst activity due to progressive catalyst deactivation. The reaction front moves downwards in the axial direction. Within the considered time range, a deterioration of the reformate gas composition was not observed with regard to the main components H_2, CO, CO_2

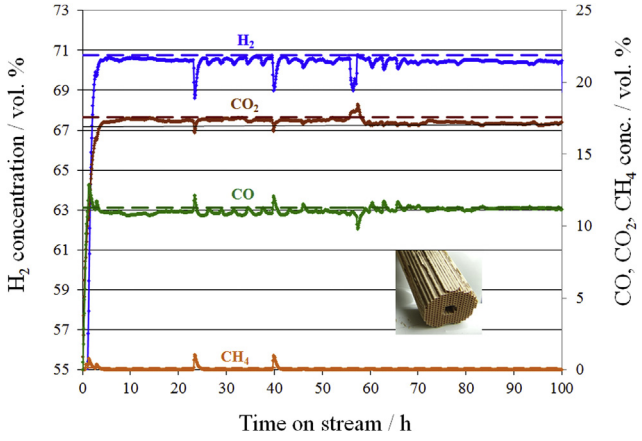

Fig. 6 – Longevity test with ceramic based catalyst monolith ($T = 800$ °C, $p = 5$ bar, S/C = 5), dry product gas composition (dotted lines: equilibrium concentrations).

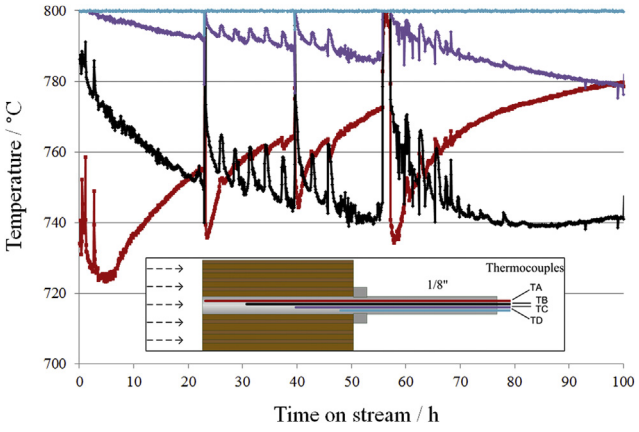

Fig. 7 – Longevity test with ceramic based catalyst monolith ($T = 800$ °C, $p = 5$ bar, S/C = 5), axial catalyst temperatures over time on stream.

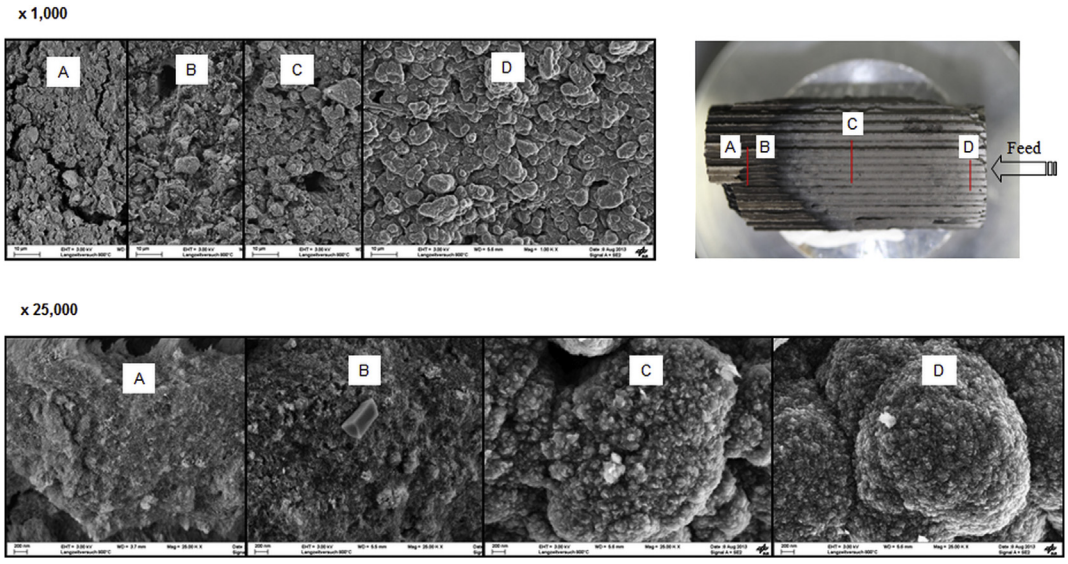

Fig. 8 – Longevity test with ceramic catalyst monolith ($T = 800$ °C, $p = 5$ bar, S/C = 5), Scanning electron microscopy of the catalyst surface.

and CH_4, since the number of active metal particles on the catalyst surface was sufficiently high to ensure equilibrium gas concentration at the catalyst outlet.

Scanning electron microscopy (SEM) and energy-dispersive X-ray spectroscopy (EDX) analysis of the catalyst surface show sintering and coking (Fig. 8). Both sintering and coking occur predominantly at the catalyst inlet, leading to a reduction of catalytically active sites for biodiesel conversion. Deactivation through coking might be caused by light hydrocarbons such as ethylene and propylene which are known to be the main precursors for coke formation [12,29]. Ethylene and propylene can be produced by thermal cracking of biodiesel or by decomposition of the fatty acids into saturated and unsaturated hydrocarbons, which can then be further converted into ethylene, propylene and other small hydrocarbons via ethylene elimination, isomerization and hydrogen transfer reactions [30]. In addition, double bonds present in the fatty acid methyl esters enhance the formation of aromatics, which are coke precursors [22]. Temperatures higher than 750 °C are necessary in order to fully convert aromatic species [21].

Notwithstanding, higher hydrocarbons have not been detected in the product gas due to sufficiently high catalyst length, allowing for a complete conversion of higher hydrocarbons into C_1 products. In contrast, during the preliminary tests at higher feed mass flow, light hydrocarbons (C_2–C_4) have been detected in 10 out of 27 experiments in the outlet stream.

It is assumed that the low temperature at the catalyst inlet is the main cause of catalyst deactivation, since this favors the evolution of light hydrocarbons and an incomplete conversion of aromatics, resulting in catalyst coking. Concurrently, Lin et al. report a deterioration of reforming efficiency as the temperature at the front end of the catalyst bed is reduced due to the application of a higher S/C [14].

Longevity test with metallic based catalyst monolith

In order to improve the long-term stability of biodiesel steam reforming, an experiment at similar conditions ($T = 840$ °C, $p = 5$ bar, S/C = 5, $m_{BD} = 5$ g/h) has been conducted using a metallic based catalyst monolith ($l = 5.1$ cm, $d = 2$ cm). The metallic catalyst substrate offers the advantage of improved heat transfer in both radial and axial directions, thus ensuring a more homogenous temperature profile.

As can be seen from Fig. 9, stable product gas composition near chemical equilibrium was achieved over 100 h. After initiation of the reforming reaction, the inlet temperature TB decreases by 38 °C (compared to 77 °C for the ceramic monolith). Moreover, catalyst temperatures in axial directions are stable during time on stream indicating high and stable catalyst activity (Fig. 10).

Analysis of the unconverted biodiesel in the cold trap revealed 98.7% biodiesel conversion. As can be seen from Fig. 11, the biodiesel peaks in the GC chromatogram have nearly vanished. 69% of the unconverted biodiesel can be attributed to coke deposits on the catalyst surface and tube walls, the remaining 31% is related to biodiesel and its cracking products. No higher hydrocarbons have been detected in the product gas.

In summary, by increasing the control temperature from 800 °C to 840 °C and using metallic instead of ceramic catalyst substrate, a significant improvement in catalyst stability could be achieved. We assume that the high temperature at the catalyst front end mitigates coke formation due to improved kinetics of the gasification reactions, in particular the reverse Boudouard reaction and the reaction of solid carbon with H_2O (Eqs. (5) and (6)). The following hypothesis is derived: As a first step, coke is formed through decomposition of biodiesel (Eq. (7)). Subsequently, the deposited coke reacts with H_2O and CO_2

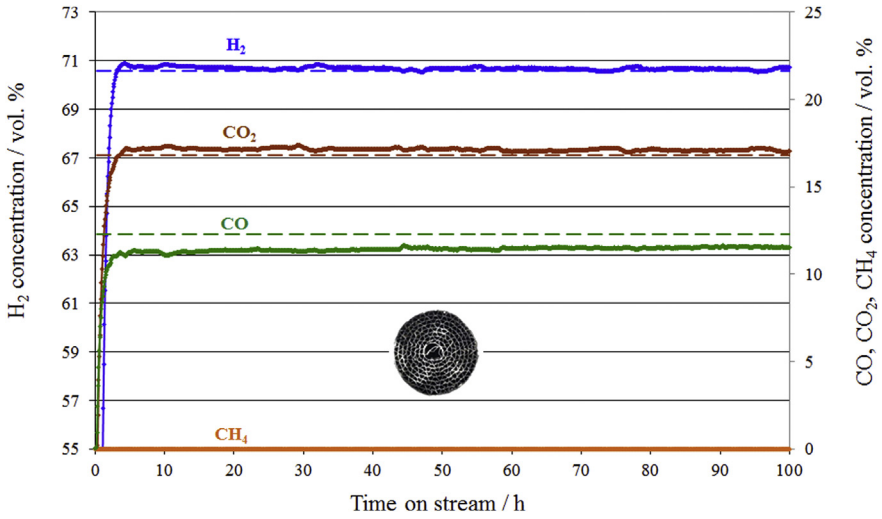

Fig. 9 – Longevity test with metallic based catalyst monolith ($T = 840$ °C, $p = 5$ bar, S/C = 5), dry product gas composition (dotted lines: equilibrium concentrations).

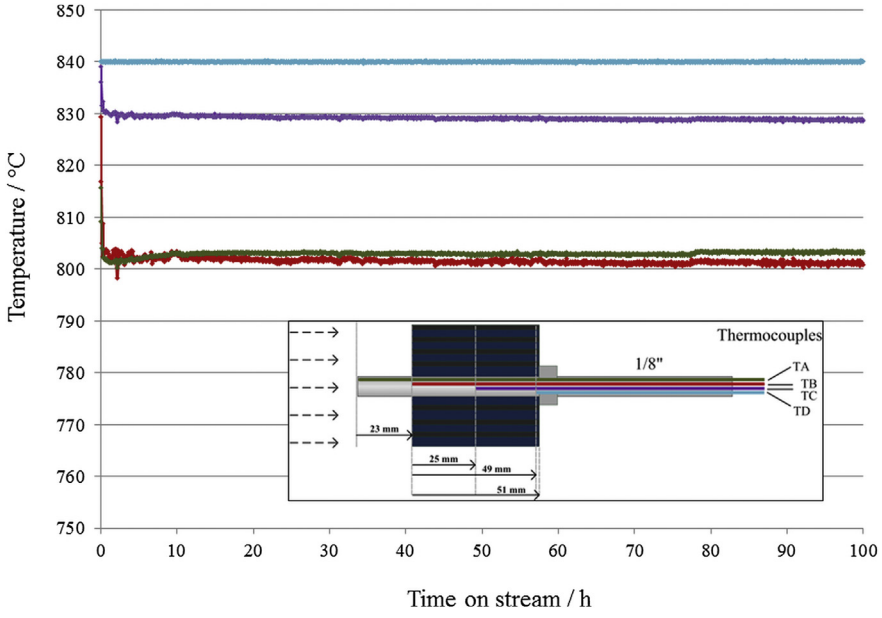

Fig. 10 – Longevity test with metallic based catalyst monolith ($T = 840$ °C, $p = 5$ bar, S/C = 5), axial catalyst temperatures over time on stream.

to CO and H_2. If the reaction rate of the gasification reactions is slower compared to the coke forming reactions in the given temperature range, this will result in an accumulation of carbon on the catalyst surface. Obviously, the accumulation is induced at the catalyst front end. The decrease of coke deposition with increasing temperature can be explained by a stronger increase of the reaction rate of gasification reactions compared to the coking reactions.

Taking into account the inverse relationship of the coking rate to coke formed [31], a drop of coking rate will be caused at the catalyst front end with time on stream. Carbon deposition then progresses in the axial direction until a point is reached where catalyst activity is significantly reduced due to a limited availability of active sites. Subsequently, reformate gas composition deteriorates, leading to an increase of methane and the evolution of light hydrocarbons. Finally, the biodiesel conversion rate decreases.

Feed mass flow variation

In order to better understand the effect of flow rate, a feed mass flow variation has been carried out. As can be seen from Fig. 12, the catalyst inlet temperature TB is stable for a biodiesel mass flow of 10 g/h over the whole temperature range,

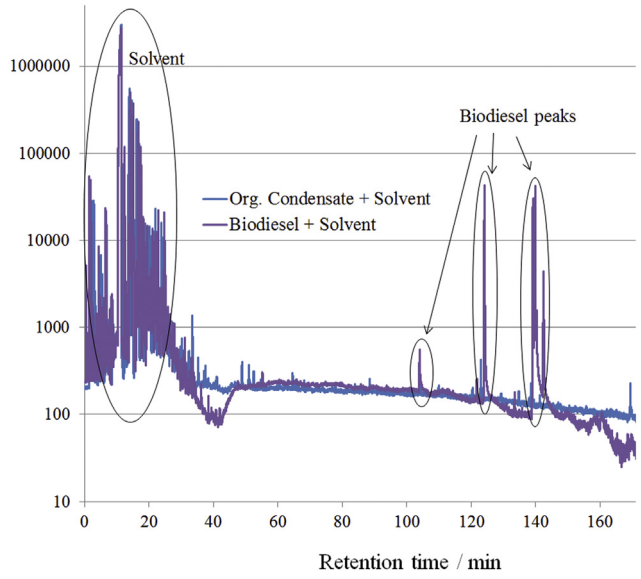

Fig. 11 – Gas chromatography analysis ($T = 840$ °C, $p = 5$ bar, S/C = 5).

indicating stable catalyst activity. In contrast, increasing the biodiesel mass flow from 10 g/h to 15 g/h results in an increase of the catalyst inlet temperature being initiated at a threshold temperature of 730 °C. When the inlet temperature is further decreased from 730 °C to 693 °C, catalyst deactivation becomes more pronounced. This finding is in line with the above-mentioned hypothesis stating that deactivation induced at the catalyst inlet is the result of kinetic limitations of the gasification reactions. At higher feed mass flows, the kinetic limitations of the reverse Boudouard reaction and the water gas reaction become more severe, resulting in a faster catalyst deactivation. Besides, formation of light hydrocarbons and aromatics is favored in the low temperature range. Thus, the observations of Lin et al. [14] and Berry [32] that high GHSV accelerates the formation of carbon can be confirmed for steam reforming of biodiesel. When comparing Fig. 12 with Fig. 7, it becomes evident that the metallic catalyst substrate shows improved performance over the ceramic substrate at similar temperature conditions. Whilst the catalyst inlet temperature remains stable at a biodiesel mass flow of 10 g/h and a temperature of 730 °C (Fig. 12), it rises sharply at a similar inlet temperature of 723 °C when using a ceramic based catalyst monolith (Fig. 7).

Conclusions

In this study, biodiesel steam reforming has been investigated at various operating conditions including variation of temperature, pressure, steam-to-carbon ratio and gas hourly space velocity. By directly mixing biodiesel at room temperature into superheated steam ($T = 550$ °C), complete vaporization of biodiesel could be ensured. Thereby, self-pyrolysis and subsequent coke formation in the mixing zone was minimized and fluctuations in reformate flow rate were avoided.

Coke deposition on the catalyst surface and sintering are determined as main causes of catalyst deactivation. Preliminary experiments using ceramic catalyst monoliths indicate increased coking tendency with decreasing temperature which is in line with literature findings and thermodynamic considerations. A longevity test at conditions where coking was found to be least severe ($T = 800$ °C, S/C = 5, $p = 5$ bar) showed a stable product gas composition. However, progressive blocking of the active sites by coke deposition occurred. By using a metallic catalyst substrate, a more homogenous

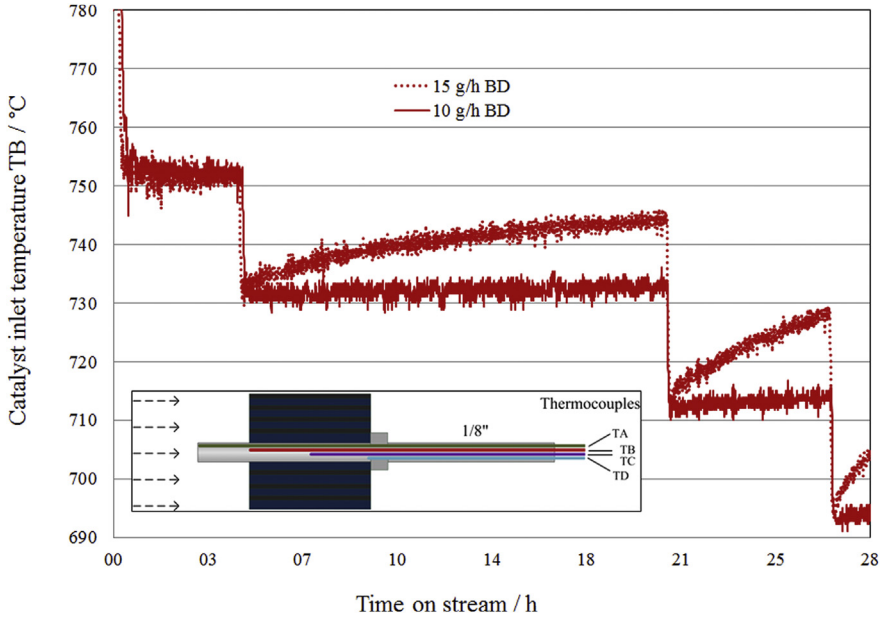

Fig. 12 – Effect of biodiesel mass flow variation on catalyst deactivation (metallic catalyst substrate, operating conditions: $p = 5$ bar, S/C = 5).

axial and radial temperature profile could be ensured, enabling higher catalyst inlet temperatures (>800 °C). Hence, coking of the catalyst was reduced to a minimum resulting in stable catalyst performance over 100 h with 99% biodiesel conversion. In addition, tests were carried out varying the feed mass flow in the temperature range 690 °C–750 °C indicating a detrimental effect of high feed mass flows on catalyst activity. The observed effect is more pronounced in the low temperature range. Moreover, the metallic based precious metal catalyst shows improved performance over the ceramic based catalyst at similar inlet temperatures.

Based on the experimental findings, it can be concluded that catalyst deactivation primarily depends on catalyst inlet conditions, in particular on inlet temperature and feed mass flow per open area of catalyst. Thus, gas hourly space velocity seems not to be an adequate parameter for determining coke formation, as catalyst length does not play a crucial role in the initiation of coking. Instead, feed mass flow per catalyst inlet area and fluid velocity are proposed as appropriate criteria for evaluating coking tendency.

The results of this study show that it is vital to ensure a minimum threshold temperature of 750 °C (assuming a feed mass flow per open area of catalyst of 31 g/h cm^2) at the catalyst inlet in order to avoid catalyst deactivation. Apart from ensuring a threshold temperature, small biodiesel flow rates are favorable in order to maintain high and stable catalyst activity. At a given catalyst inlet temperature of 730 °C a threshold mass flow of 10 g/h (corresponding to a mass flow per open area of catalyst of 21 g/h cm^2, a fluid velocity of 5 cm/s or a gas hourly space velocity of 4400 h^{-1}) must not be exceeded. Increasing the feed mass flow beyond the threshold mass flow causes immediate initiation of catalyst deactivation.

It has to be taken into account that high reformer temperatures, high steam-to-carbon ratios and low feed mass flow rates are not favorable in terms of fuel processor efficiency and system costs. Therefore a trade-off between high catalyst durability and acceptable system costs must be found.

In the present study, catalyst deactivation of biodiesel steam reforming has been studied in detail. Accordingly, optimum operating conditions have been derived. Stable biodiesel steam reforming has been shown, thus laying the basis for reformer design studies targeting commercial applications.

Acknowledgment

The authors gratefully acknowledge the support of the Fuel Cells and Hydrogen Joint Technology Initiative (FCH JU) under Grant Agreement No. 278138. The HIFUEL precious metal catalysts used in this study were kindly provided by Johnson Matthey. The biodiesel was supplied by Abengoa Bioenergy. For proofreading the manuscript we thank Martin Kraenzel.

REFERENCES

[1] Navarro Yerga RM, Alvarez-Galvan MC, Mota N, Villoria de la Mano JA, Al-Zahrani SM, Fierro JLG. Catalysts for hydrogen production from heavy hydrocarbons. ChemCatChem 2011;3:440–57.
[2] Holladay JD, Hu J, King DL, Wang Y. An overview of hydrogen production technologies. Catal Today 2009;139:244–60.
[3] Contestabile M. Analysis of the market for diesel PEM fuel cell auxiliary power units onboard long-haul trucks and of its implications for the large-scale adoption of PEM FCs. Energ Policy 2010;38:5320–34.
[4] Shukla AK, Arico AS, Antonucci V. An appraisal of electric automobile power sources. Renew Sust Energ Rev 2001;5:137–55.
[5] Levin DB, Chahine R. Challenges for renewable hydrogen production from biomass. Int J Hydrog Energy 2010;35:4962–9.
[6] Nahar G, Dupont V. Hydrogen via steam reforming of liquid biofeedstock. Biofuels 2012;3(2):167–91.
[7] Xuan J, Leung MKH, Leung DYC, Ni M. A review of biomass-derived fuel processors for fuel cell systems. Renew Sust Energ Rev 2009;13:1301–13.
[8] Diop D, Blanco M, Flammini A, Schlaifer M, Kropiwnicka MA, Mautner-Markhof M. Assessing the impact of biofuels production on developing countries from the point of view of policy coherence for development. Eur Union's Framew Contract Comm 2013;2011:23–4.
[9] Specchia S, Cutillo A, Saracco G, Specchia V. Concept study on ATR and SR fuel processors for liquid hydrocarbons. Ind Eng Chem Res 2006;45:5298–307.
[10] Martin S, Wörner A. On-board reforming of biodiesel and bioethanol for high temperature PEM fuel cells: comparison of autothermal reforming and steam reforming. J Power Sources 2011;196:3163–71.
[11] Hulteberg C. Sulphur-tolerant catalysts in small-scale hydrogen production, a review. Int J Hydrog Energy 2012;37:3978–92.
[12] Blasi A, Fiorenza G, Freda C. Steam reforming of biofuels for the production of hydrogen-rich gas. Woodhead Publishing Limited; 2014. p. 145–81.
[13] Bartholomew CH, Farrauto RJ. Fundamentals of industrial catalytic processes. 2nd ed. Wiley; 2006.
[14] Lin J, Trabold TA, Walluk MR, Smith DF. Bio-fuel reforming for solid oxide fuel cell applications. part 2: biodiesel. Int J Hydrog Energy 2014;39:183–95.
[15] Siefert NS, Shekhawat D, Smith MW, Haynes DJ, Bergen RM, Robey EH, et al. Operation of a solid oxide fuel cell on a reformed FAME mixture. Biomass Bioenerg 2012;47:362–71.
[16] Colucci JA. Hydrogen production using autothermal reforming of biodiesel and other hydrocarbons for fuel cell applications. In: ASME international solar energy conference; 2006. p. 483–4.
[17] Kraaij GJ, Specchia S, Bollito G, Mutri L, Wails D. Biodiesel fuel processor for APU applications. Int J Hydrog Energy 2009;34:4495–9.
[18] Sgroi M, Bollito G, Saracco G, Specchia SBIOFEAT. Biodiesel fuel processor for a vehicle fuel cell auxiliary power unit – study of the feed system. J Power Sources 2005;149:8–14.
[19] Specchia S, Tillemans FWA, van den Oosterkamp PF, Saracco G. Conceptual design and selection of a biodiesel fuel processor for a vehicle fuel cell auxiliary power unit. J Power Sources 2005;145:683–90.
[20] Lin J, Trabold TA, Walluk MR, Smith DF. Autothermal reforming of biodiesel-ethanol-diesel blends for solid oxide fuel cell applications. Energ Fuel 2013;27(8):4371–85.
[21] Gonzalez AV, Pettersson LJ. Full-scale autothermal reforming for transport applications: the effect of diesel fuel quality. Catal Today 2013;210:19–25.
[22] Nahar GA. Hydrogen rich gas production by the autothermal reforming of biodiesel (FAME) for utilization in the solid-oxide fuel cells: a thermodynamic analysis. Int J Hydrog Energy 2010;35:8891–911.

[23] Abatzoglou N, Fauteux-Lefebvre C, Braidy N. Biodiesel reforming with a $NiAl_2O_4/Al_2O_3$-YSZ catalyst for the production of renewable SOFC fuel. WIT Trans Ecol Environ 2011;143:145–55.
[24] Shiratori Y, Quang-Tuyen T, Umemura Y, Kitaoka T, Sasaki K. Paper-structured catalyst for the steam reforming of biodiesel fuel. Int J Hydrog Energy 2013;38:11278–87.
[25] Shiratori Y, Quang-Tuyen T, Sasaki K. Performance enhancement of biodiesel fueled SOFC using paper-structured catalyst. Int J Hydrog Energy 2013;38:9856–66.
[26] Mieville RL. Coking characteristics of reforming catalysts. J Catal 1986;100:482–8.
[27] Lin J, Trabold TA, Walluk MR, Smith DF. Bio-fuel reformation for solid oxide fuel cell applications. part 1: fuel vaporization and reactant mixing. Int J Hydrog Energy 2013;38:12024–34.
[28] Maximini M, Engelhardt P, Grote M, Brenner M. Further development of a microchannel steam reformer for diesel fuel. Int J Hydrog Energy 2012;37:10125–34.
[29] Yoon S, Kang I, Bae J. Effects of ethylene on carbon formation in diesel autothermal reforming. Int J Hydrog Energy 2008;33:4780–8.
[30] Idem RO, Katikaneni SPR, Bakhshi NN. Thermal cracking of Canola oil: reaction products in the presence and absence of steam. Energ Fuels 1996;10:1150–62.
[31] Mieville RL. Coking kinetics of reforming. Stud Surf Sci Catal 1991;68:151–9.
[32] Berry DA, Shekhawat D, Gardner TH. Development of reaction kinetics for diesel-based fuel cell reformers. American Institute of Chemical Engineers; Hydrogen, Fuel Cells and Infrastructure Technologies; 2003. FY Progress Report.